Article

Current Biology

Genetic Alzheimer's Disease Risk Affects the Neural Mechanisms of Pattern Separation in Hippocampal Subfields

Highlights

- CA3 and DG perform pattern separation in a spatial mnemonic discrimination task
- Pattern separation, but not novelty effects, are affected by APOE genotype
- APOE-ε3-ε4 and APOE-ε3-ε2 carriers show differential recruitment of CA3 and DG
- Investigating pattern separation has high potential for understanding early AD

Authors

Hweeling Lee, Rüdiger Stirnberg, Sichu Wu, ..., Sonja Jung, Christian Montag, Nikolai Axmacher

Correspondence

hweeling.lee@gmail.com

In Brief

Lee et al. show that APOE-ε3-ε3 carriers mainly recruit CA3 during a relational pattern separation task. APOE-ε3-ε4 carriers demonstrate reduced pattern separation effects in the dentate gyrus, and APOE-ε3-ε2 carriers show enhanced pattern separation effects in the CA3 and increased pattern separation-related DG-CA3 functional connectivity.

Lee et al., 2020, Current Biology *30*, 4201–4212
November 2, 2020
https://doi.org/10.1016/j.cub.2020.08.042

CellPress

Current Biology

CellPress

Article

Genetic Alzheimer's Disease Risk Affects the Neural Mechanisms of Pattern Separation in Hippocampal Subfields

Hweeling Lee,[1,7,*] Rüdiger Stirnberg,[1] Sichu Wu,[1,2] Xin Wang,[1,2,3] Tony Stöcker,[1] Sonja Jung,[4] Christian Montag,[4] and Nikolai Axmacher[5,6]

[1]German Center for Neurodegenerative Diseases (DZNE), Venusberg Campus 1, Building 99, 53127 Bonn, Germany
[2]Department of Radiology, Drum Tower Hospital, Medical School of Nanjing University, 321 Zhong Shan Road, 210008 Nanjing, China
[3]Department of Radiology, Third Affiliated Hospital of Soochow University, No. 185 Juqian Road, 213003 Changzhou, China
[4]Department of Psychology, Ulm University, Helmholtzstrasse 8/1, 89081 Ulm, Germany
[5]Department of Neuropsychology, Institute of Cognitive Neuroscience, Faculty of Psychology, Ruhr University Bochum, IB 6/185, Universitaetsstrasse 150, 44801 Bochum, Germany
[6]State Key Laboratory of Cognitive Neuroscience and Learning and IDG/McGovern Institute for Brain Research, Beijing Normal University, Xinjiekouwai Street 19, Beijing 100875, China
[7]Lead Contact
*Correspondence: hweeling.lee@gmail.com
https://doi.org/10.1016/j.cub.2020.08.042

SUMMARY

The hippocampal subfields perform distinct operations during acquisition, differentiation, and recollection of episodic memories, and deficits in pattern separation are among the first symptoms of Alzheimer's disease (AD). We investigated how hippocampal subfields contribute to pattern separation and how this is affected by Apolipoprotein-E (APOE), the strongest AD genetic risk factor. Using ultra-high-field (7T) functional magnetic resonance imaging (fMRI), APOE-ε3-ε3 carriers predominantly recruited *cornu ammonis* 3 (CA3) during a spatial mnemonic discrimination task, whereas APOE-ε3-ε4 and APOE-ε3-ε2 carriers engaged CA3 and dentate gyrus (DG) to the same degree. Specifically, APOE-ε3-ε4 carriers showed reduced pattern separation in CA3, whereas APOE-ε3-ε2 carriers exhibited increased effects in DG and pattern separation-related functional connectivity between DG and CA3. Collectively, these results demonstrate that AD genetic risk alters hemodynamic responses in young pre-symptomatic individuals, paving the way for development of biomarkers for preclinical AD.

INTRODUCTION

Memories of past experiences are crucial to guide behavior. The hippocampus is key for differentiating and recalling a specific episode among similar experiences in memory, a process called pattern separation [1–3]. However, the hippocampus consists of several histologically and functionally distinct subfields [4]. Computational models have emphasized a particular role of the dentate gyrus (DG) in pattern separation, whereas the adjacent *cornu ammonis 3* (CA3) region has been proposed to interact with the entorhinal cortex (EC) and DG to perform pattern separation or pattern completion, depending on stimulus characteristics [2, 3, 5–8]. In support of these models, animal electrophysiological recordings in rats and monkeys have shown a prominent functional contribution of DG to pattern separation, whereas CA3 has been found to support pattern completion or pattern separation [9–15].

Results from human fMRI studies are somewhat less consistent. Although distinct functions have been proposed for DG and CA3, the limited spatial resolution of blood-oxygen-level-dependent (BOLD) responses at conventional field strengths of 3T did not allow dissociation of these two areas in most studies [8, 16–18]. Even when recordings were conducted at higher resolutions (e.g., 1.5 mm^3 isotropic voxel size), DG and CA3 still remained nondissociable [19, 20]. Two recent studies using ultra-high fMRI recordings at 7T successfully dissociated the functional contributions of DG and CA3 during mnemonic discrimination and provided converging evidence that pattern separation is specifically associated with DG [21], whereas pattern completion mainly occurs in CA3 [22]. However, hypothetical CA3 pattern separation processes may be masked by simultaneously occurring memory recollection processes. Thus, classical pattern separation paradigms involving only individual items may not be optimal to probe hippocampal pattern separation processes because the hippocampus is predominantly relevant for relational memory for arbitrary associations between multiple items or between an item and its spatial location [23, 24].

Pattern separation is crucial for memory function but is also among the first cognitive functions to be affected in aging [25–28], mild cognitive impairment (MCI) [29], and Alzheimer's disease (AD) [30, 31]. Thus, one would expect neurodegeneration to occur first in the DG and/or CA3. However, histological and volumetric studies in early stages of AD demonstrate that neuronal loss and tangle accumulation within the hippocampus

A

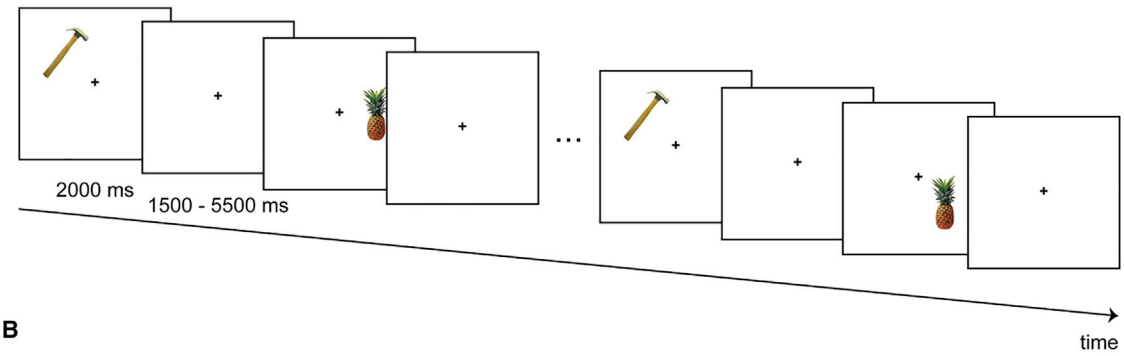

B

Response type	Stimulus type			
	foil	first	repeats	lures
"new"	correct foil	correct first	incorrect second	
"repeat"	incorrect first		correct repeats	lures "repeat"
"lure"			repeats "lure"	correct lures
no response			incorrect second	

Figure 1. Experimental Design and Trial Types

(A) During scanning, participants viewed the objects and judged whether an item was "new," "repeat," or "lure." An object was correctly judged as "new" when it was seen for the first time in the context of the task and as "repeat" when it was presented in the same location for the second time. An object was correctly judged as "lure" when it was presented again but in a different location.

(B) Summary of the regressors in the fMRI analysis. Trials were sorted post hoc according to the participants' responses using a factorial design of 4 stimulus types (foil, new, repeats, and lures) by 4 response types ("new," "repeat," "lure," and no response). Given that there were very little or no trials in some cases, trials from those conditions were collapsed into a single regressor.

are more prominent in CA1 and subiculum than in other hippocampal subfields [32–40]. To reconcile the discrepant results from studies with healthy and clinical populations, preclinical disease stages may be accessible by investigating asymptomatic genetic risk carriers. This is particularly the case in early-onset AD, which is determined by mutations of genes such as Presenilin 1 (PS1) with complete penetrance. Indeed, previous studies of asymptomatic PS1 mutation carriers demonstrated hippocampal hyperactivation during encoding of face-name associations [41] and scenes [42]. Late-onset AD is due to a combination of environmental influences and genetic risk factors, of which Apolipoprotein-E (APOE) is by far the most important [43]. The most common APOE allele, APOE-ε3, is associated with an average risk for AD, whereas the APOE-ε4 and APOE-ε2 alleles lead to a higher and a lower AD risk, respectively [43, 44]. Recent evidence suggests APOE-ε4 status to be associated with impaired pattern separation ability [31, 45, 46] and increased BOLD responses in CA3/DG during pattern separation [46]. However, these results were obtained in older African-American APOE-ε4 carriers [45, 46] or in AD patients [30, 31], leaving open the question of whether they generalize to young healthy APOE-ε4 carriers. Furthermore, given the rare occurrence of the APOE-ε2 allele in the general population, little is known about how it affects hippocampal subfield activation during pattern separation [47].

Here we addressed these questions using ultra-high-field (7T) fMRI recordings that allowed us to reliably distinguish between DG and CA3 [48]. We employed a spatial mnemonic discrimination task in which young healthy participants genotyped for APOE had to judge whether repeated items were shown at the same or at a different spatial location (Figure 1A). We hypothesized APOE genotype-specific differences in hippocampal subfield activation. Particularly, we expected neural pattern separation effects to be reduced in APOE-ε4 carriers and enhanced in APOE-ε2 carriers.

RESULTS

Eighty-two participants (33 APOE-ε3-ε3, 34 APOE-ε3-ε4, and 15 APOE-ε3-ε2 carriers; Table 1) completed a spatial mnemonic discrimination task during ultra-high-resolution fMRI at 7T (Figure 1A; STAR Methods). For every participant, trials were sorted post hoc according to a factorial design of 4 stimulus types (foils, new, repeats, and lures) by 4 responses ("new," "repeat," "lure," and no response) (Figure 1B; STAR Methods). Region of interest (ROI) masks that define the trisynaptic loop of the hippocampal formation (i.e., EC, CA1, DG, and CA3) were created and used for subsequent analyses (Figure 2; STAR Methods). We did not find any significant group effects on task performance or ROI volumes (Table 1), consistent with previous studies [29, 49].

No APOE Genetic Differences in Novelty

First we examined the effect of APOE on novelty responses in different hippocampal subfields and the EC. The novelty effect

Table 1. Summary of Demographics, ROI Volumes, and fMRI Task Performance

	APOE-ε3-ε3	APOE-ε3-ε4	APOE-ε3-ε2	$F_{(2,79)}$	p Value
n (F/M)	19/14	26/8	14/1	7.04[a]	0.03
Mean age ± S.E.M., years	22.8 ± 3.5	21.8 ± 2.1	20.8 ± 1.4	3.08	0.05
Mean Anatomical Size (across Subjects) ± SEM (mm^3)					
L. CA1	7.11 ± 0.18	6.89 ± 0.20	6.49 ± 0.19	1.80	0.17
R. CA1	7.59 ± 0.21	7.39 ± 0.21	7.46 ± 0.24	0.25	0.78
L. DG	4.98 ± 0.11	4.93 ± 0.13	4.86 ± 0.18	0.15	0.86
R. DG	5.21 ± 0.12	5.17 ± 0.14	5.33 ± 0.20	0.24	0.79
L. CA3	1.56 ± 0.05	1.54 ± 0.06	1.39 ± 0.05	1.65	0.20
R. CA3	1.63 ± 0.05	1.67 ± 0.06	1.56 ± 0.06	0.62	0.54
L. EC	9.20 ± 0.25	8.85 ± 0.23	8.81 ± 0.24	0.76	0.47
R. EC	9.04 ± 0.29	8.63 ± 0.19	8.98 ± 0.33	0.83	0.44
Mean Proportion of Responses (across Subjects) ± SEM					
Foils "new" (correct foils)	0.99 ± 0.003	.98 ± 0.007	0.99 ± 0.003	1.06	0.35
Foils "repeat"	0.00 ± 0.001	0.00 ± 0.001	0.00 ± 0.002	0.37	0.69
Foils "lure"	0.01 ± 0.003	0.01 ± 0.005	0.00 ± 0.002	1.17	0.32
Foils no response	0.00 ± 0.001	0.01 ± 0.003	0.00 ± 0.002	1.50	0.23
First "new" (correct first)	0.99 ± 0.003	0.98 ± 0.004	0.99 ± 0.003	0.75	0.48
First "repeat"	0.00 ± 0.001	0.00 ± 0.001	0.00 ± 0.001	0.44	0.64
First "lure"	0.009 ± 0.003	0.01 ± 0.003	0.01 ± 0.002	0.51	0.60
First no response	0.002 ± 0.001	0.003 ± 0.001	0.002 ± 0.001	0.46	0.63
Repeats "new"	0.04 ± 0.007	0.03 ± 0.009	0.03 ± 0.008	0.86	0.43
Repeats "repeat" (correct repeats)	0.75 ± 0.03	0.78 ± 0.02	0.77 ± 0.04	0.36	0.70
Repeats "lure"	0.21 ± 0.02	0.19 ± 0.02	0.20 ± 0.03	0.24	0.79
Repeats no response	0.01 ± 0.002	0.01 ± 0.003	0.00 ± 0.002	1.11	0.34
Lures "new"	0.04 ± 0.007	0.03 ± 0.009	0.03 ± 0.007	0.09	0.92
Lures "repeat"	0.23 ± 0.01	0.25 ± 0.01	0.23 ± 0.01	0.96	0.39
Lures "lure" (correct lures)	0.72 ± 0.02	0.70 ± 0.01	0.73 ± 0.02	1.13	0.33
Lures no response	0.01 ± 0.002	0.01 ± 0.004	0.01 ± 0.002	1.40	0.25

Demographics, mean anatomical size (in square millimeters) for each ROI, and mean proportion of responses were calculated for a factorial design of 4 stimulus types (foils, new, repeats, and lure) by 4 responses ("new," "repeat," "lure," and no response) in each genotype group. One-way ANOVAs were performed for every item listed. See also Table S2.

[a]Non-parametric Kruskal-Wallis test was performed to test for number of males versus females in the genotype groups.

was defined as the contrast between correctly identified new stimuli (i.e., correct new) compared with correctly recognized repeated items (i.e., correct repeats). Consistent with previous ultra-high-field studies [21, 51, 52], we averaged the parameter estimates of the two hemispheres in each ROI. Figure 3A shows boxplots for the mean parameter estimates of the novelty effect (see also Figures S1A and S2A for novelty effects for each hemisphere and for each sex, respectively). An analysis of covariance (ANCOVA) (STAR Methods) revealed a significant main effect of "ROI" ($F_{(2,1,\ 159.6)} = 3.1$, $p = 0.048$). We did not observe any main effects of "group" ($F_{(2,\ 77)} = 0.8$, $p = 0.5$) or the covariates "age" ($F_{(1,\ 77)} = 1.7$, $p = 0.2$) and "sex" ($F_{(1,\ 77)} = 0.01$, $p = 0.9$). There were no significant interactions between "ROI" and the covariate "age" ($F_{(2.1,\ 159.6)} = 0.9$, $p = 0.4$), "ROI" and the covariate "sex" ($F_{(2.1,\ 159.6)} = 1.8$, $p = 0.2$), or "ROI" and "group" ($F_{(4.1,\ 159.6)} = 0.2$, $p = 0.97$).

Pooled across the APOE genotype groups, follow-up paired-sample t tests comparing novelty effects between ROIs yielded significant differences for CA3 > DG ($t_{(81)} = 7.10$, $p < 0.001$), CA3 > CA1 ($t_{(81)} = 8.44$, $p < 0.001$), CA3 > EC ($t_{(81)} = 10.0$, $p < 0.001$), CA1 > DG ($t_{(81)} = 2.79$, $p = 0.007$), CA1 > EC ($t_{(81)} = 5.85$, $p < 0.001$), and DG > EC ($t_{(81)} = 6.79$, $p < 0.001$) (Figure 4). Collectively, the results demonstrate the strongest novelty effect in CA3, followed by CA1 and DG, and the weakest novelty effect in EC (i.e., CA3 > CA1 > DG > EC).

Pattern Separation Effects in the DG and CA3 Show APOE Genetic Differences

Next we examined APOE genotype effects on pattern separation in different hippocampal subfields and the EC. Similar to previous studies [18, 28, 46, 53, 54], pattern separation was identified via the contrast of correctly identified lure stimuli (i.e., correct lures) as compared to lure stimuli that were incorrectly identified as "repeat" (i.e., lures "repeat"). This contrast compares the two response conditions under which the lure stimulus has been remembered correctly (otherwise participants would have

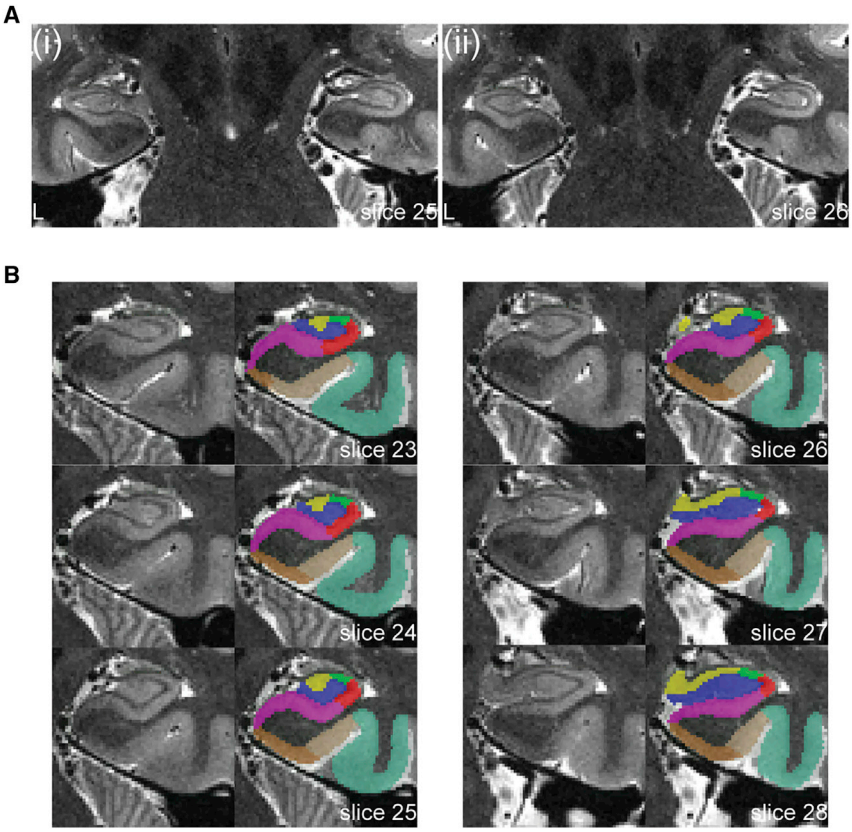

Figure 2. Hippocampal Subfields and the EC

(A) T2-weighted images of a single subject showing (i) the posterior end of the hippocampal head and (ii) the anterior start of the hippocampal body. Medial temporal lobe (MTL) regions and hippocampal subfields were automatically segmented based on T1- and T2-weighted images using the automated segmentation of hippocampal subfields (ASHS) procedure [48] with an atlas template created by Berron et al. [50]. The segmentation results from all participants were subsequently verified manually.

(B) Slice-by-slice segmentation of results of the ASHS procedure (examples from slices 23–28). Slices are 1.1 mm apart. Included are the entorhinal cortex (EC; brown), perirhinal cortex (area 35 in light brown, area 36 in mint green), subiculum (magenta), *cornu ammonis* 1 (CA1; red), CA2 (green), CA3 (yellow), and dentate gyrus (DG; blue). Functional ROIs were created for the EC, CA1, CA3, and DG.

responded "new"), but only under the "correct lures" condition was the location correctly identified as new. In other words, this contrast attempts to isolate the process of interest while keeping other processes the same. Figure 3B shows boxplots for the mean parameter estimates of the pattern separation effect (see also Figures S1B and S2B for pattern separation effects for each hemisphere and for each sex, respectively). Interestingly, an ANCOVA (STAR Methods) revealed a significant main effect of "group" ($F_{(2, 77)} = 4.1$, $p = 0.02$) and a significant interaction between "ROI" and "group" ($F_{(4.6, 178.0)} = 3.2$, $p = 0.01$). We did not observe significant main effects of "ROI" ($F_{(2.3, 178.0)} = 0.6$, $p = 0.6$) or the covariates "age" ($F_{(1, 77)} = 0.08$, $p = 0.8$) and "sex" ($F_{(1, 77)} = 0.01$, $p = 0.9$). There were no significant interactions of "ROI" and the covariate "age" ($F_{(2.3, 178.0)} = 0.6$, $p = 0.6$) or "ROI" and the covariate "sex" ($F_{(2.3, 178.0)} = 1.0$, $p = 0.4$). Furthermore, when we modeled each of the lure conditions as a separate regressor and re-calculated the pattern separation effects (Figure S3; STAR Methods), we did not find any significant interactions of "lure type" and "ROI" ($F_{(5.6, 427.6)} = 1.06$, $p = 0.38$), "lure type" and "group" ($F_{(4.8, 186.2)} = 1.35$, $p = 0.25$), or "lure type," "ROI," and "group" [$F_{(11.1, 427.6)} = 0.96$, $p = 0.49$), indicating that the interaction of "ROI" and "group" observed in our main analysis was not affected by the difficulty level of the lures.

Follow-up univariate analyses of APOE genotype effects in each ROI revealed significant group effects in DG ($F_{(2, 79)} = 5.78$, $p = 0.005$) and CA3 ($F_{(2, 79)} = 4.88$, $p = 0.01$) but not in EC ($F_{(2, 79)} = 0.74$, $p = 0.48$) or CA1 ($F_{(2, 79)} = 2.03$, $p = 0.14$). We thus focused our analyses on DG and CA3. Paired-sample t tests comparing the mean pattern separation-related parameter estimates in DG versus CA3 demonstrated a stronger pattern separation effect in CA3 relative to DG in APOE-ε3-ε3 carriers ($t_{(32)} = 2.50$, $p = 0.02$). This result was not found in APOE-ε3-ε4 carriers ($t_{(33)} = 0.36$, $p = 0.72$) or in APOE-ε3-ε2 carriers ($t_{(14)} = 0.83$, $p = 0.42$). In other words, APOE-ε3-ε3 carriers predominantly recruited CA3 rather than DG for pattern separation, whereas APOE-ε3-ε4 and APOE-ε3-ε2 carriers used CA3 and DG regions to a similar degree.

We next tested whether the differences between the APOE genotype groups were due to reduced recruitment of CA3 by APOE-ε3-ε4 and APOE-ε3-ε2 carriers and/or due to enhanced recruitment of DG. Pairwise comparisons between the 3 APOE genotype groups in CA3 revealed reduced pattern separation effects in APOE-ε3-ε4 relative to APOE-ε3-ε3 carriers ($t_{(65)} = -2.53$, $p = 0.01$) and APOE-ε3-ε2 carriers ($t_{(47)} = -2.51$, $p = 0.02$) (Figure 3B(iv)). There was no difference between APOE-ε3-ε3 relative to APOE-ε3-ε2 carriers ($t_{(65)} = -0.86$, $p = 0.40$). In contrast, DG showed enhanced pattern separation effects in APOE-ε3-ε2 relative to APOE-ε3-ε3 carriers ($t_{(46)} = 2.68$, $p = 0.01$) and APOE-ε3-ε4 carriers ($t_{(47)} = 3.30$, $p = 0.002$) (Figure 3B(iii)). Importantly, however, there was no difference between APOE-ε3-ε4 and APOE-ε3-ε3 carriers ($t_{(65)} = -1.18$, $p = 0.24$). Together, these results show higher levels of activity in CA3 than DG during relational pattern separation in APOE-ε3-ε3 carriers. They further demonstrate that, although APOE-ε3-ε4 and APOE-ε3-ε2 carriers recruited CA3 and DG to the same degree, APOE-ε3-ε4 carriers, compared with APOE-ε3-ε3 carriers, showed lower recruitment of CA3 but no difference in DG recruitment. In contrast, APOE-ε3-ε2 carriers, compared with APOE-ε3-ε3 carriers, showed higher recruitment of DG but no difference in CA3 recruitment.

Some previous studies identified pattern separation by comparing correct lures with correct repeats [16, 55]. However, this contrast did not yield any significant APOE genotype effects (Figure S4). Conceptually, this contrast is less suitable for our

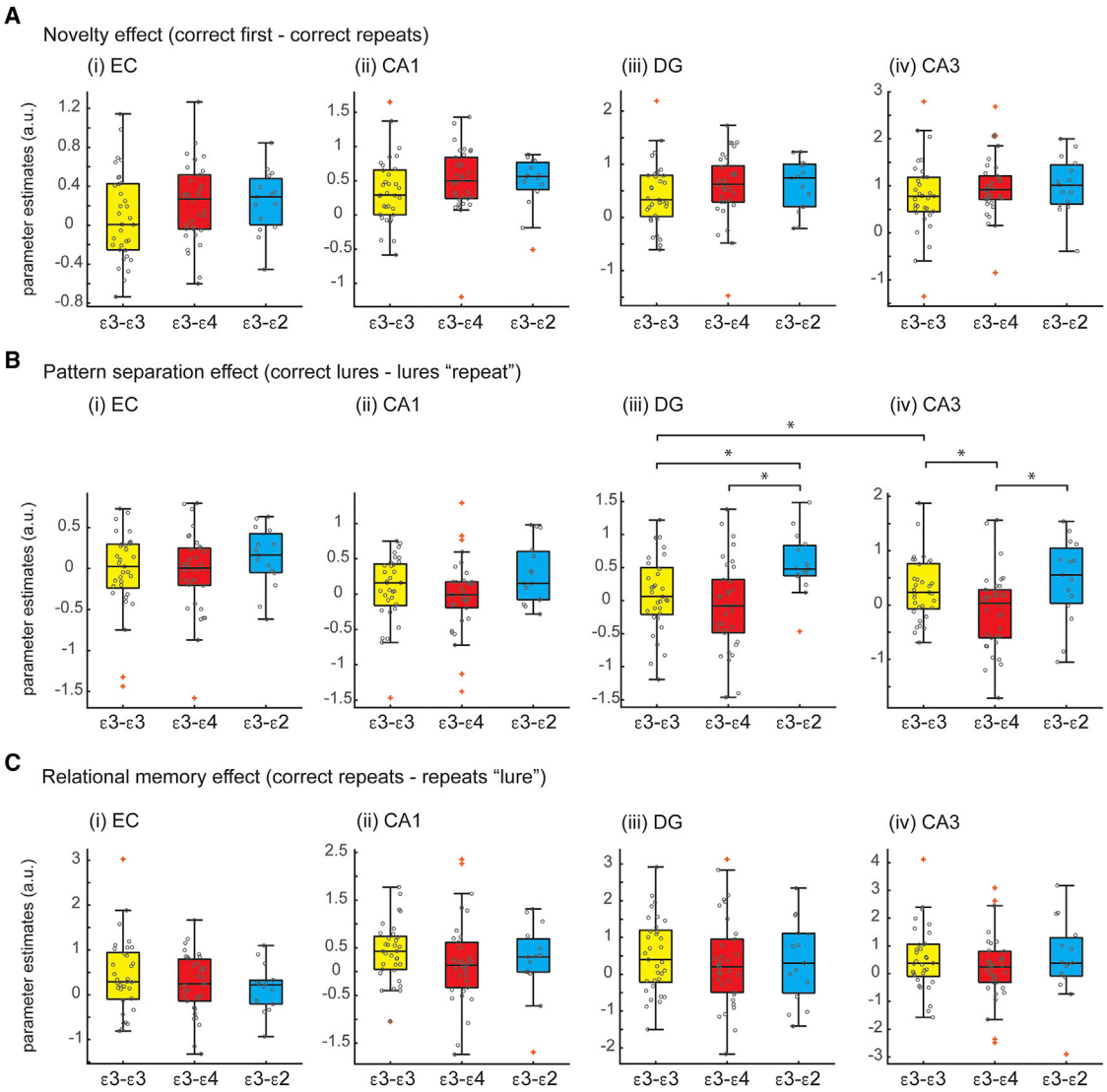

Figure 3. Novelty, Pattern Separation, and Relational Memory Effects in Hippocampal Subfields and the EC

Boxplots of mean (across subjects) parameter estimates of (A) novelty (i.e., correct first-correct repeats), (B) pattern separation (i.e., correct lures-lures "repeat"), and (C) relational memory (i.e., correct repeats-repeats "lure") in the (i) EC, (ii) CA1, (iii) DG, and (iv) CA3 for APOE-ε3-ε3 carriers (yellow bars), APOE-ε3-ε4 carriers (red bars), and APOE-ε3-ε2 carriers (blue bars). Orange crosses indicate outliers, and gray circles indicate individual subjects' values. *p < 0.05. The scales differ between plots. See also Figures S1–S4.

paradigm because correct repeats and correct lures reflect trials in which participants successfully remembered the previously presented item and also recognized whether the associated spatial location had been shown before. Thus, both conditions could be considered to reflect successful source memory, and they only differ in whether a novel or a repeated location was correctly identified.

No APOE Differences in Relational Memory

Following our analysis approach, "correct repeats" trials involve recognition of an item as old and accurate recall of its spatial location context, whereas context recall failed for repeat trials that were incorrectly identified as a "lure" (i.e., repeats "lure"), indicating a lack of relational memory. Figure 3C shows boxplots for the mean parameter estimates of relational memory (i.e., correct repeats-repeats "lure"). An ANCOVA (STAR Methods) revealed significant main effects of "ROI" ($F_{(2.3,\ 171.8)} = 3.31$, $p = 0.03$) and the covariate "age" ($F_{(1,\ 77)} = 4.99$, $p = 0.03$) and a significant interaction of "ROI" and the covariate "age" ($F_{(2.3,\ 171.8)} = 3.25$, $p = 0.04$). There were no significant main effects of "group" ($F_{(2,\ 77)} = 0.83$, $p = 0.44$) or the covariate "sex" ($F_{(1,\ 77)} = 1.44$, $p = 0.23$). There were also no significant interactions of "ROI" and "group" ($F_{(4.5,\ 171.8)} = 0.42$, $p = 0.82$) or "ROI" and the covariate "sex" ($F_{(2.3,\ 171.8)} = 0.73$, $p = 0.50$).

Since the covariate "age" has a significant effect on "ROI," we performed multiple ANCOVAs to compare the effects among the ROIs, pooled across groups while controlling for the covariate "age." For comparison of CA3 with EC, we found a significant

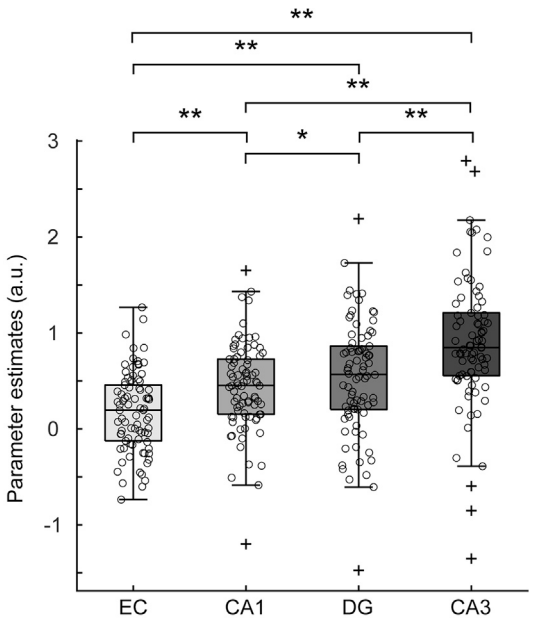

Figure 4. Novelty Effects in Hippocampal Subfields and the EC

Boxplot of mean (across subjects) parameter estimates, pooled across groups, of novelty (i.e., correct first-correct repeat) in hippocampal subfields and the EC. Black crosses indicate outliers, and black circles indicate individual subjects' values. *p < 0.01, ** p < 0.001.

main effect of "ROI" ($F_{(1.0,\ 80.0)} = 5.0$, p = 0.03), indicating a more pronounced relational memory effect in CA3 than EC, and a significant interaction of "ROI" and the covariate "age" ($F_{(1.0,\ 80.0)} = 4.6$, p = 0.04) but no main effect of the covariate "age" ($F_{(1,\ 80)} = 2.9$, p = 0.09). For comparison of CA1 with DG, we found a trend for a main effect of "ROI" ($F_{(1.0,\ 80.0)} = 3.4$, p = 0.07) with a stronger relational memory effect in DG relative to CA1 but no main effect of the covariate "age" ($F_{(1,\ 80)} = 2.1$, p = 0.15) and no interaction of "ROI" and the covariate "age" ($F_{(1.0,\ 80.0)} = 2.7$, p = 0.11) was observed. For comparison of CA1 with CA3, we found a significant main effect of "ROI" ($F_{(1.0,\ 80.0)} = 4.9$, p = 0.03) with a stronger relational memory effect in CA3 relative to CA1, a trend for a main effect of the covariate "age" ($F_{(1,\ 80)} = 3.5$, p = 0.07), and a significant interaction of "ROI" and the covariate "age" ($F_{(1.0,\ 80.0)} = 4.3$, p = 0.04). For comparison of DG with EC, we found a marginally significant main effect of "ROI" ($F_{(1.0,\ 80.0)} = 3.6$, p = 0.06) with a stronger relational memory effect for EC relative to DG, but no main effect of the covariate "age" ($F_{(1,\ 80)} = 1.5$, p = 0.22) or interaction of "ROI" and the covariate "age" ($F_{(1.0,\ 80.0)} = 3.2$, p = 0.08) was observed. For comparison of CA1 with EC, we did not find any significant main effect of "ROI" ($F_{(1.0,\ 80.0)} = 0.78$, p = 0.38), the covariate "age" ($F_{(1,\ 80)} = 0.62$, p = 0.44), or interaction of "ROI" and the covariate "age" ($F_{(1.0,\ 80.0)} = 82$, p = 0.37). Finally, for comparison of DG with CA3, we found a significant main effect of the covariate "age" ($F_{(1,\ 80)} = 4.1$, p = 0.045), but no main effect of "ROI" ($F_{(1.0,\ 80.0)} = 0.89$, p = 0.35) or interaction of "ROI" and the covariate "age" ($F_{(1.0,\ 80.0)} = 90$, p = 0.35) was observed. Together, these analyses show the most pronounced relational memory effect within the CA3 region, consistent with previous studies (e.g., McNaughton and Morris [2]). Importantly, no significant APOE genotype differences on relational memory were observed.

Pattern Separation-Related Functional Connectivity between the DG and CA3 Depends on APOE

We tested whether APOE genotype effects on pattern separation were associated with differences in the functional connectivity (FC) between hippocampal subregions, which could possibly drive compensatory increases or decreases in regional recruitment. We used beta-series correlation analyses [56] to calculate pattern separation-related FC in the hippocampal formation (STAR Methods). Figure 5 shows boxplots of pattern separation-related FC (i.e., correct lures-lures "repeat") for all 6 connectivities.

An ANCOVA (STAR Methods) revealed a significant main effect of "connectivity" ($F_{(2.7,204.1)} = 4.80$, p = 0.004) and a marginally significant main effect of the covariate "sex" ($F_{(1,77)} = 3.72$, p = 0.06) but no main effect of the covariate "age" ($F_{(1,77)} = 2.63$, p = 0.11) or "group" ($F_{(2,77)} = 0.10$, p = 0.91). Importantly, there was also a significant interaction of "connectivity" and "group" ($F_{(5.3,204.1)} = 2.50$, p = 0.03). There were also significant interactions between "connectivity" and the covariates "sex" ($F_{(2.7,204.1)} = 4.84$, p = 0.004) and "age" ($F_{(2.7,204.1)} = 3.61$, p = 0.02). We thus performed pairwise comparisons of the 3 APOE genotype groups for each connectivity while controlling for the covariates "sex" and "age" (Table S1). Interestingly, DG-CA3 FC was reduced for APOE-ε3-ε4 relative to APOE-ε3-ε2 carriers ($F_{(1,\ 45)} = 4.64$, p = 0.04) but did not differ between APOE-ε3-ε3 and APOE-ε3-ε4 carriers ($F_{(1,\ 63)} = 1.24$, p = 0.27) or between APOE-ε3-ε2 and APOE-ε3-ε3 carriers ($F_{(1,\ 44)} = 2.41$, p = 0.13). The other connectivities did not differ between the different genotype groups. Post hoc paired t tests comparing DG-CA3 FC for correct lures versus lure "repeats" in APOE-ε3-ε4 carriers (Figure 6A) did not show a difference between the two conditions ($t_{(33)} = -1.56$, p = 0.13) and showed a trend between the two conditions in APOE-ε3-ε2 carriers (Figure 6B) ($t_{(14)} = 1.96$, p = 0.07).

DISCUSSION

In the current study, we examined the functional contribution of different subregions of the hippocampal formation to pattern separation in a spatial mnemonic discrimination task and how this is affected by APOE genotype. We identified differential novelty effects across the hippocampal formation, with the strongest novelty effect in CA3 followed by CA1 and DG and the weakest novelty effect in EC. Novelty effects did not depend on APOE genotype. In addition, we found pattern separation effects in CA3 and DG that were affected by APOE genotype, and this effect was not influenced by sex. Interestingly, APOE-ε3-ε3 carriers predominantly recruited CA3 rather than DG. APOE-ε3-ε4 carriers recruited CA3 to a lesser degree than APOE-ε3-ε3 carriers but did not differ in DG recruitment. In contrast, APOE-ε3-ε2 carriers showed higher recruitment of DG relative to APOE-ε3-ε3 carriers but no difference in CA3 activation. APOE-ε3-ε2 carriers further exhibited a trend of higher FC between DG and CA3 during successful versus failed pattern separation, unlike APOE-ε3-ε3 carriers. Collectively, our results indicate that, although APOE-ε3-ε4 and APOE-ε3-ε2 carriers recruit DG and CA3 to the same degree, this pattern results from

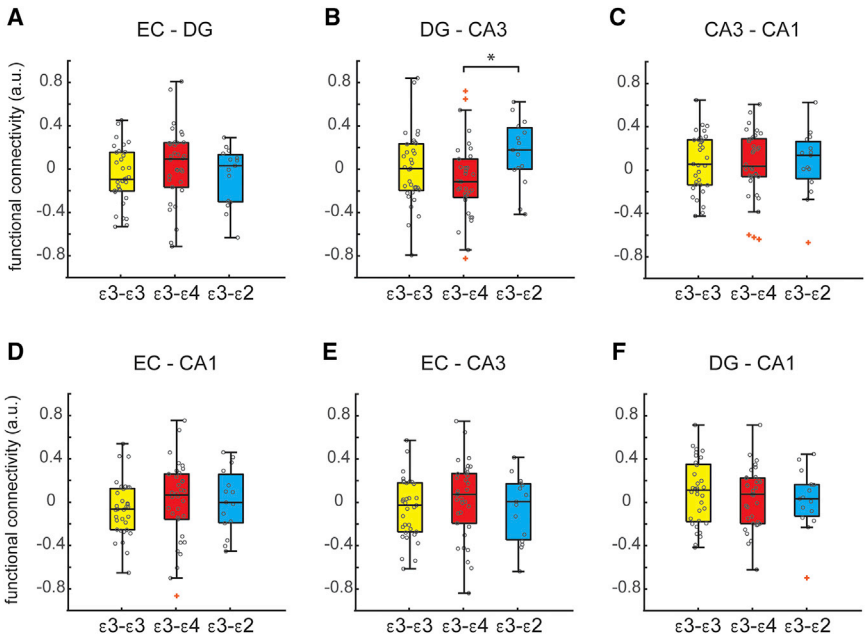

Figure 5. Pattern Separation-Related FC

Boxplots of mean (across subjects) parameter estimates of pattern separation-related (i.e., correct lures-lures "repeat") FC in (A) EC-DG, (B) DG-CA3, (C) CA3-CA1, (D) EC-CA1, (E) EC-CA3, and (F) DG-CA1 for APOE-ε3-ε3 carriers (yellow bars), APOE-ε3-ε4 carriers (red bars), and APOE-ε3-ε2 carriers (blue bars). Orange crosses indicate outliers, and gray circles indicate individual subjects' values. *$p < 0.05$. See also Table S1.

different alterations to the recruitment profile observed in APOE-ε3-ε3 carriers.

In our study, we found the strongest novelty effect in CA3, followed by CA1 and DG, and the weakest novelty effect in EC. Our results diverge from previous findings that suggest that either CA1 plays the most important role in novelty processing [57] or that all hippocampal subregions contribute to novelty processing to a similar degree [58]. One could speculate that BOLD responses mainly measure synaptic inputs [59] and recurrent processing [60] within an area, the latter of which is particularly abundant in the CA3. Direct electrophysiological recordings would be required to clarify this issue and elucidate the mapping between BOLD responses and electrophysiology in the hippocampus (e.g., Kunz et al. [61]). Interestingly, we did not find any APOE genotype effect on novelty in the hippocampal formation. This differs from previous neuroimaging studies that reported reduced medial temporal lobe (MTL) activation in response to novel stimuli in AD patients [62–65] and increased activation in MCI patients [63, 66]. It is well possible that the effects in patients with more advanced pathology are still masked in the healthy participants at risk investigated here. Furthermore, because of the relational nature of our paradigm, initial formation of an association between an item and its spatial position may require pronounced recruitment of the recurrent network of the CA3 area (to form the association). In other words, it may not be the detection of novelty per se but, rather, the formation of novel associations that induces the strongest activation of the CA3 region in our data.

Our results further demonstrate that BOLD responses in CA3 and DG and the FC between DG and CA3 are influenced by APOE genotype. Importantly, these effects are observed in APOE-ε3-ε4 carriers who are at high AD risk but do not yet exhibit any age-related deficits in pattern separation [20, 29, 31, 45, 46]. Our current findings demonstrate a reduced pattern separation effect in CA3 in APOE-ε3-ε4 carriers and enhancement of pattern separation effects in DG in APOE-ε3-ε2 carriers. Although theoretical models and previous empirical work suggest a predominant role of DG in pattern separation (of similar individual items), we found the most prominent activation in CA3 rather than in DG in APOE-ε3-ε3 carriers. At the current stage, we do not have a comprehensive explanation for why CA3 rather than DG appears to support pattern separation in our paradigm. Some previous studies have shown a role of the CA3 region in pattern separation of relatively dissimilar stimuli or changes in spatial location (e.g., Yassa and Stark [8] and Leutgeb et al. [67]). It is possible that "detonator" mossy fiber synapses support all-or-none activation of small assemblies of recurrently connected CA3 cells, which may be required for representation of item-context associations [1, 2]. Specifically, the correct response to a lure in our paradigm requires recognition of an item as one that has been presented previously and identification of its spatial location as new, and such recall of item-location associations is typically linked to the CA3 region. Thus, selective recruitment of such assemblies may be particularly relevant for pattern separation of item-location associations, whereas pattern separation of individual items may occur in the DG region.

Our findings also demonstrate the highest degree of DG-CA3 FC in APOE-ε3-ε2 carriers and the lowest degree of DG-CA3 FC in APOE-ε3-ε4 carriers, whereas the degree of DG-CA3 FC in APOE-ε3-ε3 carriers does not differ significantly from the two other groups. Based on the univariate results, one may have expected to find a lower degree of DG-CA3 FC in APOE-ε3-ε3 carriers because pattern separation-related effects in DG and CA3 differ in this group, whereas they do not differ in the other two groups. However, averaged activity across trials and correlations between trials are independent measures. In other words, the same overall amounts of activity in DG and CA3 (as measured by condition-specific regressors in the general linear model (GLM) we used for univariate analyses) may be associated with completely different levels of inter-trial correlations. At the physiological level, FC is typically interpreted as indicating inter-regional information transfer [68] or (in a pathological framework) as a spread of pathology, functional compensatory changes in recruitment, or decoupling of pathologically altered areas. Given the differences in AD risk between the three groups, we tentatively suggest that a high degree of DG-CA3 FC reflects a beneficial (physiological) information transfer that is reduced in

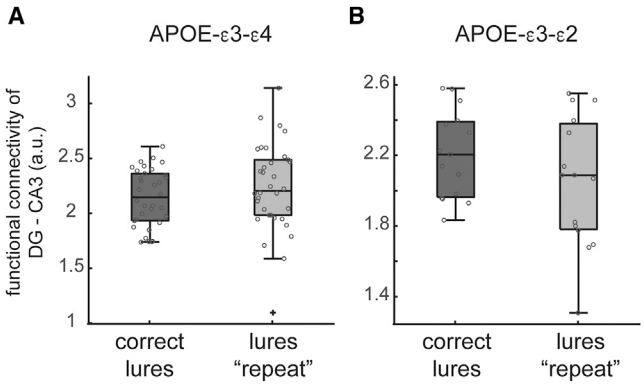

Figure 6. Pattern Separation-Related FC between DG and CA3

Boxplots of mean (across subjects) FC of DG-CA3 for correct lures (dark gray bars) and lures "repeat" (light gray bars) in (A) APOE-ε3-ε4 carriers and (B) APOE-ε3-ε2 carriers. Black crosses indicate outliers, and gray circles indicate individual subjects' values.

APOE-ε3-ε4 carriers, possibly also reflecting decoupling of physiologically impaired subregions of the hippocampus in an attempt to avoid the spread of pathology [69–72]. We note that these interpretations need to remain speculative at the current stage.

Our analysis strategy differed substantially from the approach adopted in several previous neuroimaging studies on pattern separation [8, 16, 18, 20, 21, 28, 29]. In the analysis of pattern separation, we compared "correct lures" trials with lure trials in which participants gave an incorrect "repeat" response (i.e., lures "repeat"). It may be argued that failure to give a correct response may be due to various reasons; e.g., participants were less attentive in some trials, did not completely process the perceptual information in a stimulus, or pressed a wrong button. Although we cannot completely rule out that these factors contributed in some cases, it is unlikely that they completely explain the responses under the lures "repeat" condition, for two reasons. First, we found that, under the most difficult lure condition (i.e., when the locations of the items only differed by ±22.5° from the original location of the item [lure1]), the proportion of "repeat" responses was significantly higher compared with the second most difficult lure condition (i.e., when the locations of the items differed by ±45° from the original location of the item [lure2]) (Table S2). These results suggest that participants are more likely to incorrectly respond "repeat" to a lure item when pattern separation demands are higher. This pattern of results would not be expected if participants just pressed an incorrect button or did not pay attention at all. Second, as described above, the correct response to a lure in our paradigm requires two processes: recognition of an item as one that has been presented previously and identification of its spatial location as new. The first process could be conceived as item-based recognition memory, whereas the second requires pattern separation. For lure items that are incorrectly identified as "repeat," the first but not the second process is applied successfully. This suggests that participants paid at least some degree of attention to these trials. Our analysis recapitulates analyses in previous relational memory studies in which trials with correct item and source responses were compared with trials in which only an item was remembered but not its associated source [73–75]. Our results suggest that this relational version of pattern separation depends on a different hippocampal subregion (CA3) compared with conventional, object-based pattern separation (DG) [21]. Future studies should directly compare these effects, ideally by employing both paradigms in the same participants.

Although the majority of previous pattern separation studies focused on pattern separation of individual items, several previous studies in rodents and humans also investigated spatial versions of pattern separation paradigms. For example, a recent study provided evidence of a behaviorally relevant role of the hippocampus in separating neural representations of specific environments using multivariate analyses of fMRI data [76]. In addition, other studies investigating impairment of spatial pattern separation related to aging and AD showed that although healthy elderly participants did not show overall deficits in spatial pattern separation, a subgroup of elderly participants with impaired memory exhibited reduced spatial pattern completion ability [26]. Such deficits were also found in healthy elderly APOE-ε4 carriers [45], and the deficits in MCI patients correlated with hippocampal and entorhinal volumes [77]. In addition, rodent studies using similar experimental paradigms allowed investigation of regional contributions and cellular mechanisms in greater detail (e.g., Gilbert et al. [78], Hunsaker et al. [79], and Yeates et al. [80]).

Although studies of early-onset AD patients consistently reported hippocampal hyperactivation that likely reflects early pathology [41, 42], results from APOE-ε4 carriers of late-onset AD are less consistent. Some studies showed reduced [81, 82] and other studies enhanced [83–85] hippocampal activity in APOE-ε4 carriers during memory encoding. Hyperactivity in APOE-ε4 carriers may reflect very early pathology or functional compensatory attempts (which may be maladaptive) [86]. Computer simulations suggest that such hyperactivity may arise from excessive pattern completion and insufficient pattern separation, resulting in "runaway" synaptic modification [87]. Our findings further demonstrate that, despite differences in hippocampal BOLD responses between APOE genotype groups, these groups did not differ in behavioral performance. APOE-related BOLD differences despite normal performance have been reported in several previous studies on young presymptomatic APOE-ε4 carriers [29, 49]. For example, using a spatial navigation paradigm, we found strongly impaired "grid cell-like representations" in the EC of APOE-ε3-ε4 carriers compared with APOE-ε3-ε3 carriers [70]. Importantly, however, APOE-ε4 carriers were not impaired in this task, suggesting that alterations of regional BOLD activity patterns may precede behavioral impairments. A similar divergence of APOE-ε4-related BOLD alterations in the absence of any behavioral impairments was also found in several other studies (e.g., Adamson et al. [81], Konishi et al. [88], and Rajah et al. [89]). Consistent with previous studies, we suggest that alterations of BOLD responses despite normal behavioral performance may be explained by subclinical pathological processes or functional compensation (or both; i.e., functional compensatory attempts that induce pathology in the long term; see, e.g., Jagust and Mormino [90]). Because the participants in our study are rather young, it is probably more likely that activation differences reflect functional compensatory changes rather than actual neuropathology. In

addition, the causal factors linking the APOE-ε4 genotype to BOLD activity levels in DG remain unclear and need to be addressed in future studies. In particular, it will be important to test whether these activity differences are associated with AD pathology (as measured via, e.g., cerebrospinal fluid (CSF) biomarkers or amyloid and tau PET imaging). Because APOE-ε4 is also a prominent vascular risk factor, it will be crucial to test whether the reduced BOLD responses may be due to alterations in neurovascular coupling or reflect changes of neural activity. Whereas neurovascular coupling may be investigated via advanced imaging techniques such as vascular space occupancy (VASO) [91], intracranial electroencephalogram (EEG) recordings in epilepsy patients (genotyped for APOE) may be used to address the latter question.

The current study has several limitations. First, the number of participants in the APOE-ε3-ε2 group was relatively small compared with the APOE-ε3-ε3 and APOE-ε3-ε4 groups. This is due to the rather low frequency of APOE-ε2 carriers, who account for only about 8% of the general population [43, 47]. Second, the ratios of males and females were imbalanced in the APOE genotype groups. The possibility that sex differences might confound the results was reduced by controlling for possible effects of sex (using sex as a covariate) in all statistical models. Nevertheless, future studies with more balanced sex ratios should more exhaustively explore possible effects of sex. Third, the clinical relevance of the current results in relation to AD remains unclear because young healthy participants were recruited for the study. Future studies should investigate elderly participants who are at different stages of AD development (e.g., those who are healthy, show subjective cognitive decline or pre-MCI, amnestic MCI, and mild AD) and test whether APOE genotype is a predictive factor for pattern separation abilities. Fourth, the question of whether differences in pattern separation neural representation observed in the APOE genotype groups will persist and affect memory later in life needs to be addressed in future longitudinal studies.

In conclusion, using a spatial mnemonic discrimination task during high-resolution 7T fMRI scanning allowed us to differentiate the contribution of hippocampal subregions to relational pattern separation and its modulation by APOE genotype. This approach may complement traditional neuropsychological tests and spatial navigation tasks [92] as research paradigms for understanding preclinical AD and predicting disease progression. In addition, future studies should also explore the relationship between the neurocognitive basis of pattern separation, neuropsychological, and psychometric tests.

STAR★METHODS

Detailed methods are provided in the online version of this paper and include the following:

- KEY RESOURCES TABLE
- RESOURCE AVAILABILITY
  - Lead Contact
  - Materials Availability
  - Data and Code Availability
- EXPERIMENTAL MODEL AND SUBJECT DETAILS
- METHOD DETAILS
  - Spatial mnemonic discrimination task
  - MRI data acquisition
- QUANTIFICATION AND STATISTICAL ANALYSIS
  - Hippocampal subfields segmentation
  - Behavioral analyses
  - fMRI data preprocessing and analyses
  - Functional connectivity analyses

SUPPLEMENTAL INFORMATION

Supplemental Information can be found online at https://doi.org/10.1016/j.cub.2020.08.042.

ACKNOWLEDGMENTS

The authors would like to thank Oliver Speck and Myung Ho In for providing the PSF-EPI sequence; Yilmaz Sagik, Anke Ruehling, and Lukas Kunz for subject recruitment and data collection; and Michael Wagner and Verena Heise for reviewing the manuscript. N.A. received funding from the Deutsche Forschungsgemeinschaft (DFG; German Research Foundation) Projektnummer 316803389 – SFB 1280 and Projektnummer 122679504 – SFB 874.

AUTHOR CONTRIBUTIONS

H.L. and N.A. designed the experiments. H.L., R.S., and T.S. conducted the experiments. H.L., S.W., and X.W. analyzed the data. S.J. and C.M. performed APOE genotyping analyses. H.L. and N.A. wrote the manuscript. R.S., T.S., S.J., C.M., S.W., and X.W. edited the manuscript.

DECLARATION OF INTERESTS

The authors declare no competing interests.

Received: March 26, 2020
Revised: June 30, 2020
Accepted: August 11, 2020
Published: September 10, 2020

REFERENCES

1. Hasselmo, M.E., and Wyble, B.P. (1997). Free recall and recognition in a network model of the hippocampus: simulating effects of scopolamine on human memory function. Behav. Brain Res. *89*, 1–34.
2. McNaughton, B.L., and Morris, R.G. (1987). Hippocampal synaptic enhancement and information storage within a distributed memory system. Trends Neurosci. *10*, 408–415.
3. Treves, A., and Rolls, E.T. (1994). Computational analysis of the role of the hippocampus in memory. Hippocampus *4*, 374–391.
4. Duvernoy, H.M. (2005). The human hippocampus, Functional Anatomy, Vascularization, and Serial Sections with MRI, Third Edition (Springer).
5. Marr, D. (1971). Simple memory: a theory for archicortex. Philos. Trans. R. Soc. Lond. B Biol. Sci. *262*, 23–81.
6. O'Reilly, R.C., and McClelland, J.L. (1994). Hippocampal conjunctive encoding, storage, and recall: avoiding a trade-off. Hippocampus *4*, 661–682.
7. Treves, A., Tashiro, A., Witter, M.P., and Moser, E.I. (2008). What is the mammalian dentate gyrus good for? Neuroscience *154*, 1155–1172.
8. Yassa, M.A., and Stark, C.E. (2011). Pattern separation in the hippocampus. Trends Neurosci. *34*, 515–525.
9. Kesner, R.P., Hunsaker, M.R., and Warthen, M.W. (2008). The CA3 subregion of the hippocampus is critical for episodic memory processing by means of relational encoding in rats. Behav. Neurosci. *122*, 1217–1225.
10. Lee, H., Wang, C., Deshmukh, S.S., and Knierim, J.J. (2015). Neural Population Evidence of Functional Heterogeneity along the CA3

Transverse Axis: Pattern Completion versus Pattern Separation. Neuron *87*, 1093–1105.

11. Leutgeb, J.K., Leutgeb, S., Moser, M.B., and Moser, E.I. (2007). Pattern separation in the dentate gyrus and CA3 of the hippocampus. Science *315*, 961–966.
12. Madar, A.D., Ewell, L.A., and Jones, M.V. (2019). Pattern separation of spiketrains in hippocampal neurons. Sci. Rep. *9*, 5282.
13. Neunuebel, J.P., and Knierim, J.J. (2012). Spatial firing correlates of physiologically distinct cell types of the rat dentate gyrus. J. Neurosci. *32*, 3848–3858.
14. Neunuebel, J.P., and Knierim, J.J. (2014). CA3 retrieves coherent representations from degraded input: direct evidence for CA3 pattern completion and dentate gyrus pattern separation. Neuron *81*, 416–427.
15. Sakon, J.J., and Suzuki, W.A. (2019). A neural signature of pattern separation in the monkey hippocampus. Proc. Natl. Acad. Sci. USA *116*, 9634–9643.
16. Bakker, A., Kirwan, C.B., Miller, M., and Stark, C.E. (2008). Pattern separation in the human hippocampal CA3 and dentate gyrus. Science *319*, 1640–1642.
17. Deuker, L., Doeller, C.F., Fell, J., and Axmacher, N. (2014). Human neuroimaging studies on the hippocampal CA3 region - integrating evidence for pattern separation and completion. Front. Cell. Neurosci. *8*, 64.
18. Yassa, M.A., Stark, S.M., Bakker, A., Albert, M.S., Gallagher, M., and Stark, C.E. (2010). High-resolution structural and functional MRI of hippocampal CA3 and dentate gyrus in patients with amnestic Mild Cognitive Impairment. Neuroimage *51*, 1242–1252.
19. Bonnici, H.M., Chadwick, M.J., Kumaran, D., Hassabis, D., Weiskopf, N., and Maguire, E.A. (2012). Multi-voxel pattern analysis in human hippocampal subfields. Front. Hum. Neurosci. *6*, 290.
20. Yassa, M.A., Mattfeld, A.T., Stark, S.M., and Stark, C.E. (2011). Age-related memory deficits linked to circuit-specific disruptions in the hippocampus. Proc. Natl. Acad. Sci. USA *108*, 8873–8878.
21. Berron, D., Schütze, H., Maass, A., Cardenas-Blanco, A., Kuijf, H.J., Kumaran, D., and Düzel, E. (2016). Strong Evidence for Pattern Separation in Human Dentate Gyrus. J. Neurosci. *36*, 7569–7579.
22. Grande, X., Berron, D., Horner, A.J., Bisby, J.A., Düzel, E., and Burgess, N. (2019). Holistic Recollection via Pattern Completion Involves Hippocampal Subfield CA3. J. Neurosci. *39*, 8100–8111.
23. Eichenbaum, H., Yonelinas, A.P., and Ranganath, C. (2007). The medial temporal lobe and recognition memory. Annu. Rev. Neurosci. *30*, 123–152.
24. Henke, K. (2010). A model for memory systems based on processing modes rather than consciousness. Nat. Rev. Neurosci. *11*, 523–532.
25. Holden, H.M., and Gilbert, P.E. (2012). Less efficient pattern separation may contribute to age-related spatial memory deficits. Front. Aging Neurosci. *4*, 9.
26. Stark, S.M., Yassa, M.A., and Stark, C.E. (2010). Individual differences in spatial pattern separation performance associated with healthy aging in humans. Learn. Mem. *17*, 284–288.
27. Wilson, I.A., Gallagher, M., Eichenbaum, H., and Tanila, H. (2006). Neurocognitive aging: prior memories hinder new hippocampal encoding. Trends Neurosci. *29*, 662–670.
28. Yassa, M.A., Lacy, J.W., Stark, S.M., Albert, M.S., Gallagher, M., and Stark, C.E. (2011). Pattern separation deficits associated with increased hippocampal CA3 and dentate gyrus activity in nondemented older adults. Hippocampus *21*, 968–979.
29. Stark, S.M., Yassa, M.A., Lacy, J.W., and Stark, C.E. (2013). A task to assess behavioral pattern separation (BPS) in humans: Data from healthy aging and mild cognitive impairment. Neuropsychologia *51*, 2442–2449.
30. Ally, B.A., Hussey, E.P., Ko, P.C., and Molitor, R.J. (2013). Pattern separation and pattern completion in Alzheimer's disease: evidence of rapid forgetting in amnestic mild cognitive impairment. Hippocampus *23*, 1246–1258.
31. Wesnes, K.A., Annas, P., Basun, H., Edgar, C., and Blennow, K. (2014). Performance on a pattern separation task by Alzheimer's patients shows possible links between disrupted dentate gyrus activity and apolipoprotein E ∈4 status and cerebrospinal fluid amyloid-β42 levels. Alzheimers Res. Ther. *6*, 20.
32. Apostolova, L.G., Dutton, R.A., Dinov, I.D., Hayashi, K.M., Toga, A.W., Cummings, J.L., and Thompson, P.M. (2006). Conversion of mild cognitive impairment to Alzheimer disease predicted by hippocampal atrophy maps. Arch. Neurol. *63*, 693–699.
33. Bobinski, M., de Leon, M.J., Tarnawski, M., Wegiel, J., Reisberg, B., Miller, D.C., and Wisniewski, H.M. (1998). Neuronal and volume loss in CA1 of the hippocampal formation uniquely predicts duration and severity of Alzheimer disease. Brain Res. *805*, 267–269.
34. Kerchner, G.A., Deutsch, G.K., Zeineh, M., Dougherty, R.F., Saranathan, M., and Rutt, B.K. (2012). Hippocampal CA1 apical neuropil atrophy and memory performance in Alzheimer's disease. Neuroimage *63*, 194–202.
35. Kerchner, G.A., Hess, C.P., Hammond-Rosenbluth, K.E., Xu, D., Rabinovici, G.D., Kelley, D.A., Vigneron, D.B., Nelson, S.J., and Miller, B.L. (2010). Hippocampal CA1 apical neuropil atrophy in mild Alzheimer disease visualized with 7-T MRI. Neurology *75*, 1381–1387.
36. La Joie, R., Perrotin, A., de La Sayette, V., Egret, S., Doeuvre, L., Belliard, S., Eustache, F., Desgranges, B., and Chételat, G. (2013). Hippocampal subfield volumetry in mild cognitive impairment, Alzheimer's disease and semantic dementia. Neuroimage Clin. *3*, 155–162.
37. Rössler, M., Zarski, R., Bohl, J., and Ohm, T.G. (2002). Stage-dependent and sector-specific neuronal loss in hippocampus during Alzheimer's disease. Acta Neuropathol. *103*, 363–369.
38. Schönheit, B., Zarski, R., and Ohm, T.G. (2004). Spatial and temporal relationships between plaques and tangles in Alzheimer-pathology. Neurobiol. Aging *25*, 697–711.
39. Trujillo-Estrada, L., Dávila, J.C., Sánchez-Mejias, E., Sánchez-Varo, R., Gomez-Arboledas, A., Vizuete, M., Vitorica, J., and Gutiérrez, A. (2014). Early neuronal loss and axonal/presynaptic damage is associated with accelerated amyloid-β accumulation in AβPP/PS1 Alzheimer's disease mice subiculum. J. Alzheimers Dis. *42*, 521–541.
40. West, M.J., Coleman, P.D., Flood, D.G., and Troncoso, J.C. (1994). Differences in the pattern of hippocampal neuronal loss in normal ageing and Alzheimer's disease. Lancet *344*, 769–772.
41. Quiroz, Y.T., Budson, A.E., Celone, K., Ruiz, A., Newmark, R., Castrillón, G., Lopera, F., and Stern, C.E. (2010). Hippocampal hyperactivation in presymptomatic familial Alzheimer's disease. Ann. Neurol. *68*, 865–875.
42. Quiroz, Y.T., Willment, K.C., Castrillon, G., Muniz, M., Lopera, F., Budson, A., and Stern, C.E. (2015). Successful Scene Encoding in Presymptomatic Early-Onset Alzheimer's Disease. J. Alzheimers Dis. *47*, 955–964.
43. Liu, C.C., Liu, C.C., Kanekiyo, T., Xu, H., and Bu, G. (2013). Apolipoprotein E and Alzheimer disease: risk, mechanisms and therapy. Nat. Rev. Neurol. *9*, 106–118.
44. Shen, L., and Jia, J. (2016). An Overview of Genome-Wide Association Studies in Alzheimer's Disease. Neurosci. Bull. *32*, 183–190.
45. Sheppard, D.P., Graves, L.V., Holden, H.M., Delano-Wood, L., Bondi, M.W., and Gilbert, P.E. (2016). Spatial pattern separation differences in older adult carriers and non-carriers for the apolipoprotein E epsilon 4 allele. Neurobiol. Learn. Mem. *129*, 113–119.
46. Sinha, N., Berg, C.N., Tustison, N.J., Shaw, A., Hill, D., Yassa, M.A., and Gluck, M.A. (2018). APOE ε4 status in healthy older African Americans is associated with deficits in pattern separation and hippocampal hyperactivation. Neurobiol. Aging *69*, 221–229.
47. Suri, S., Heise, V., Trachtenberg, A.J., and Mackay, C.E. (2013). The forgotten APOE allele: a review of the evidence and suggested mechanisms for the protective effect of APOE ε2. Neurosci. Biobehav. Rev. *37*, 2878–2886.
48. Yushkevich, P.A., Pluta, J.B., Wang, H., Xie, L., Ding, S.L., Gertje, E.C., Mancuso, L., Kliot, D., Das, S.R., and Wolk, D.A. (2015). Automated volumetry and regional thickness analysis of hippocampal subfields and

medial temporal cortical structures in mild cognitive impairment. Hum. Brain Mapp. *36*, 258–287.

49. Jack, C.R., Jr., Petersen, R.C., Xu, Y.C., O'Brien, P.C., Waring, S.C., Tangalos, E.G., Smith, G.E., Ivnik, R.J., Thibodeau, S.N., and Kokmen, E. (1998). Hippocampal atrophy and apolipoprotein E genotype are independently associated with Alzheimer's disease. Ann. Neurol. *43*, 303–310.
50. Berron, D., Vieweg, P., Hochkeppler, A., Pluta, J.B., Ding, S.L., Maass, A., Luther, A., Xie, L., Das, S.R., Wolk, D.A., et al. (2017). A protocol for manual segmentation of medial temporal lobe subregions in 7 Tesla MRI. Neuroimage Clin. *15*, 466–482.
51. Hodgetts, C.J., Voets, N.L., Thomas, A.G., Clare, S., Lawrence, A.D., and Graham, K.S. (2017). Ultra-High-Field fMRI Reveals a Role for the Subiculum in Scene Perceptual Discrimination. J. Neurosci. *37*, 3150–3159.
52. Suthana, N.A., Donix, M., Wozny, D.R., Bazih, A., Jones, M., Heidemann, R.M., Trampel, R., Ekstrom, A.D., Scharf, M., Knowlton, B., et al. (2015). High-resolution 7T fMRI of Human Hippocampal Subfields during Associative Learning. J. Cogn. Neurosci. *27*, 1194–1206.
53. Kirwan, C.B., and Stark, C.E. (2007). Overcoming interference: an fMRI investigation of pattern separation in the medial temporal lobe. Learn. Mem. *14*, 625–633.
54. Wais, P.E., Jahanikia, S., Steiner, D., Stark, C.E.L., and Gazzaley, A. (2017). Retrieval of high-fidelity memory arises from distributed cortical networks. Neuroimage *149*, 178–189.
55. Lacy, J.W., Yassa, M.A., Stark, S.M., Muftuler, L.T., and Stark, C.E. (2010). Distinct pattern separation related transfer functions in human CA3/dentate and CA1 revealed using high-resolution fMRI and variable mnemonic similarity. Learn. Mem. *18*, 15–18.
56. Rissman, J., Gazzaley, A., and D'Esposito, M. (2004). Measuring functional connectivity during distinct stages of a cognitive task. Neuroimage *23*, 752–763.
57. Lisman, J.E., and Grace, A.A. (2005). The hippocampal-VTA loop: controlling the entry of information into long-term memory. Neuron *46*, 703–713.
58. Maass, A., Schütze, H., Speck, O., Yonelinas, A., Tempelmann, C., Heinze, H.J., Berron, D., Cardenas-Blanco, A., Brodersen, K.H., Stephan, K.E., and Düzel, E. (2014). Laminar activity in the hippocampus and entorhinal cortex related to novelty and episodic encoding. Nat. Commun. *5*, 5547.
59. Logothetis, N.K., Pauls, J., Augath, M., Trinath, T., and Oeltermann, A. (2001). Neurophysiological investigation of the basis of the fMRI signal. Nature *412*, 150–157.
60. Logothetis, N.K. (2008). What we can do and what we cannot do with fMRI. Nature *453*, 869–878.
61. Kunz, L., Maidenbaum, S., Chen, D., Wang, L., Jacobs, J., and Axmacher, N. (2019). Mesoscopic Neural Representations in Spatial Navigation. Trends Cogn. Sci. *23*, 615–630.
62. Bastin, C., Delhaye, E., Moulin, C., and Barbeau, E.J. (2019). Novelty processing and memory impairment in Alzheimer's disease: A review. Neurosci. Biobehav. Rev. *100*, 237–249.
63. Dickerson, B.C., Salat, D.H., Greve, D.N., Chua, E.F., Rand-Giovannetti, E., Rentz, D.M., Bertram, L., Mullin, K., Tanzi, R.E., Blacker, D., et al. (2005). Increased hippocampal activation in mild cognitive impairment compared to normal aging and AD. Neurology *65*, 404–411.
64. Golby, A., Silverberg, G., Race, E., Gabrieli, S., O'Shea, J., Knierim, K., Stebbins, G., and Gabrieli, J. (2005). Memory encoding in Alzheimer's disease: an fMRI study of explicit and implicit memory. Brain *128*, 773–787.
65. Sperling, R.A., Bates, J.F., Chua, E.F., Cocchiarella, A.J., Rentz, D.M., Rosen, B.R., Schacter, D.L., and Albert, M.S. (2003). fMRI studies of associative encoding in young and elderly controls and mild Alzheimer's disease. J. Neurol. Neurosurg. Psychiatry *74*, 44–50.
66. Dickerson, B.C., Salat, D.H., Bates, J.F., Atiya, M., Killiany, R.J., Greve, D.N., Dale, A.M., Stern, C.E., Blacker, D., Albert, M.S., and Sperling, R.A. (2004). Medial temporal lobe function and structure in mild cognitive impairment. Ann. Neurol. *56*, 27–35.
67. Leutgeb, S., Leutgeb, J.K., Treves, A., Moser, M.B., and Moser, E.I. (2004). Distinct ensemble codes in hippocampal areas CA3 and CA1. Science *305*, 1295–1298.
68. Eickhoff, S.B., and Müller, V.I. (2015). Functional Connectivity. In Brain Mapping, A.W. Toga, ed. (Academic Press), pp. 187–201.
69. Clément, F., and Belleville, S. (2010). Compensation and disease severity on the memory-related activations in mild cognitive impairment. Biol. Psychiatry *68*, 894–902.
70. Kunz, L., Schröder, T.N., Lee, H., Montag, C., Lachmann, B., Sariyska, R., Reuter, M., Stirnberg, R., Stöcker, T., Messing-Floeter, P.C., et al. (2015). Reduced grid-cell-like representations in adults at genetic risk for Alzheimer's disease. Science *350*, 430–433.
71. Scheller, E., Peter, J., Schumacher, L.V., Lahr, J., Mader, I., Kaller, C.P., and Klöppel, S. (2017). APOE moderates compensatory recruitment of neuronal resources during working memory processing in healthy older adults. Neurobiol. Aging *56*, 127–137.
72. Weis, S., Leube, D., Erb, M., Heun, R., Grodd, W., and Kircher, T. (2011). Functional neuroanatomy of sustained memory encoding performance in healthy aging and in Alzheimer's disease. Int. J. Neurosci. *121*, 384–392.
73. Lee, H., Stirnberg, R., Stöcker, T., and Axmacher, N. (2017). Audiovisual integration supports face-name associative memory formation. Cogn. Neurosci. *8*, 177–192.
74. Staresina, B.P., and Davachi, L. (2009). Mind the gap: binding experiences across space and time in the human hippocampus. Neuron *63*, 267–276.
75. Staresina, B.P., Michelmann, S., Bonnefond, M., Jensen, O., Axmacher, N., and Fell, J. (2016). Hippocampal pattern completion is linked to gamma power increases and alpha power decreases during recollection. eLife *5*, e17397.
76. Kyle, C.T., Stokes, J.D., Lieberman, J.S., Hassan, A.S., and Ekstrom, A.D. (2015). Successful retrieval of competing spatial environments in humans involves hippocampal pattern separation mechanisms. eLife *4*, e10499.
77. Parizkova, M., Lerch, O., Andel, R., Kalinova, J., Markova, H., Vyhnalek, M., Hort, J., and Laczó, J. (2020). Spatial Pattern Separation in Early Alzheimer's Disease. J. Alzheimers Dis. *76*, 121–138.
78. Gilbert, P.E., Kesner, R.P., and Lee, I. (2001). Dissociating hippocampal subregions: double dissociation between dentate gyrus and CA1. Hippocampus *11*, 626–636.
79. Hunsaker, M.R., Rosenberg, J.S., and Kesner, R.P. (2008). The role of the dentate gyrus, CA3a,b, and CA3c for detecting spatial and environmental novelty. Hippocampus *18*, 1064–1073.
80. Yeates, D.C.M., Ussling, A., Lee, A.C.H., and Ito, R. (2020). Double dissociation of learned approach-avoidance conflict processing and spatial pattern separation along the dorsoventral axis of the dentate gyrus. Hippocampus *30*, 596–609.
81. Adamson, M.M., Hutchinson, J.B., Shelton, A.L., Wagner, A.D., and Taylor, J.L. (2011). Reduced hippocampal activity during encoding in cognitively normal adults carrying the APOE ε4 allele. Neuropsychologia *49*, 2448–2455.
82. Mondadori, C.R., de Quervain, D.J., Buchmann, A., Mustovic, H., Wollmer, M.A., Schmidt, C.F., Boesiger, P., Hock, C., Nitsch, R.M., Papassotiropoulos, A., et al. (2007). Better memory and neural efficiency in young apolipoprotein E epsilon4 carriers. Cereb. Cortex *17*, 1934–1947.
83. Bondi, M.W., Houston, W.S., Eyler, L.T., and Brown, G.G. (2005). fMRI evidence of compensatory mechanisms in older adults at genetic risk for Alzheimer disease. Neurology *64*, 501–508.
84. Bookheimer, S.Y., Strojwas, M.H., Cohen, M.S., Saunders, A.M., Pericak-Vance, M.A., Mazziotta, J.C., and Small, G.W. (2000). Patterns of brain activation in people at risk for Alzheimer's disease. N. Engl. J. Med. *343*, 450–456.
85. Filippini, N., MacIntosh, B.J., Hough, M.G., Goodwin, G.M., Frisoni, G.B., Smith, S.M., Matthews, P.M., Beckmann, C.F., and Mackay, C.E. (2009). Distinct patterns of brain activity in young carriers of the APOE-epsilon4 allele. Proc. Natl. Acad. Sci. USA *106*, 7209–7214.

86. Palop, J.J., and Mucke, L. (2016). Network abnormalities and interneuron dysfunction in Alzheimer disease. Nat. Rev. Neurosci. *17*, 777–792.

87. Hasselmo, M.E. (1994). Runaway synaptic modification in models of cortex: Implications for Alzheimer's disease. Neural Netw. *7*, 13–40.

88. Konishi, K., Joober, R., Poirier, J., MacDonald, K., Chakravarty, M., Patel, R., Breitner, J., and Bohbot, V.D. (2018). Healthy versus Entorhinal Cortical Atrophy Identification in Asymptomatic APOE4 Carriers at Risk for Alzheimer's Disease. J. Alzheimers Dis. *61*, 1493–1507.

89. Rajah, M.N., Wallace, L.M.K., Ankudowich, E., Yu, E.H., Swierkot, A., Patel, R., Chakravarty, M.M., Naumova, D., Pruessner, J., Joober, R., et al. (2017). Family history and APOE4 risk for Alzheimer's disease impact the neural correlates of episodic memory by early midlife. Neuroimage Clin. *14*, 760–774.

90. Jagust, W.J., and Mormino, E.C. (2011). Lifespan brain activity, β-amyloid, and Alzheimer's disease. Trends Cogn. Sci. *15*, 520–526.

91. Huber, L., Ivanov, D., Handwerker, D.A., Marrett, S., Guidi, M., Uludağ, K., Bandettini, P.A., and Poser, B.A. (2018). Techniques for blood volume fMRI with VASO: From low-resolution mapping towards sub-millimeter layer-dependent applications. Neuroimage *164*, 131–143.

92. Coughlan, G., Laczó, J., Hort, J., Minihane, A.M., and Hornberger, M. (2018). Spatial navigation deficits - overlooked cognitive marker for preclinical Alzheimer disease? Nat. Rev. Neurol. *14*, 496–506.

93. Montag, C., Kunz, L., Axmacher, N., Sariyska, R., Lachmann, B., and Reuter, M. (2014). Common genetic variation of the APOE gene and personality. BMC Neurosci. *15*, 64.

94. Zaitsev, M., Hennig, J., and Speck, O. (2004). Point spread function mapping with parallel imaging techniques and high acceleration factors: fast, robust, and flexible method for echo-planar imaging distortion correction. Magnetic resonance in medicine *52*, 1156–1166.

95. In, M.H., and Speck, O. (2012). Highly accelerated PSF-mapping for EPI distortion correction with improved fidelity. MAGMA *25*, 183–192.

96. Di, X., Zhang, Z., and Biswal, B.B. (2020). Understanding psychophysiological interaction and its relations to beta series correlation. Brain Imaging Behav. Published online July 24, 2020. https://doi.org/10.1007/s11682-020-00304-8.

STAR★METHODS

KEY RESOURCES TABLE

REAGENT or RESOURCE	SOURCE	IDENTIFIER
Deposited Data		
fMRI data	This paper	Available on request
Software and Algorithms		
MATLAB 2018b	MathWorks	https://www.mathworks.com/products/matlab.html
Presentation	Neurobehavioral systems	https://www.neurobs.com/menu_presentation/menu_features/features_overview
Statistical Parametric Mapping (SPM12)	Wellcome Trust Centre for Neuroimaging	https://www.fil.ion.ucl.ac.uk/spm/
Statistical Package for Social Sciences (SPSS)	UNICOM	https://www.ibm.com/products/spss-statistics
Other		
7T (MAGNETOM) magnetic resonance imaging research scanner	Siemens Healthineers	Siemens Healthineers, Erlangen, Germany

RESOURCE AVAILABILITY

Lead Contact

Further information and requests for resources should be directed to and will be fulfilled by the Lead Contact, Hweeling Lee (hweeling.lee@gmail.com).

Materials Availability

This study did not generate new unique reagents.

Data and Code Availability

The dataset supporting the current study has not been deposited in a public repository due to restrictions on data sharing in our ethical approval, and as the participants did not consent to sharing their data publicly. However, fully anonymized data can be shared upon request.

EXPERIMENTAL MODEL AND SUBJECT DETAILS

Eight hundred and forty young healthy adults gave informed consent and provided buccal swap samples for APOE genotyping (genotyping procedures are as in Montag et al. [93]). Three hundred and ten participants were then randomly selected based on their APOE genotype (APOE-ε3-ε4, APOE-ε3-ε3, or APOE-ε3-ε2), and recalled to check their willingness and suitability to participate in the fMRI experiment. One hundred and seven young healthy adults participated in the fMRI experiment, but 7 datasets were discarded from further analyses (3 due to data transfer failure, 2 due to data collection error and 2 due to poor structural segmentation of the hippocampal subfields).

Of the 100 participants, a further 18 datasets were discarded from further analyses because of relatively large movements during fMRI data collection compared to the fMRI spatial resolution (mean framewise displacement across the 2 sessions > 0.5 mm). Eighty-two datasets were thus included in the final analyses. During the period of data collection, we tried our best to recruit similar proportions of males and females. However, the iterative procedure of double-blind selection of candidates, invitation to the scanning sessions and quality control of the acquired data did not allow us to completely balance the ratio of male to female participants in the individual APOE genotype groups. Univariate analysis for age revealed a significant group effect [$F_{(2,79)} = 3.08$, $p = 0.05$], with APOE-ε3-ε3 carriers being slightly older than APOE-ε3-ε2 carriers [$t_{(46)} = 2.12$, $p = 0.04$]. APOE-ε3-ε4 carriers did not differ in age from either APOE-ε3-ε3 carriers [$t_{(65)} = -1.41$, $p = 0.16$] or APOE-ε3-ε2 carriers [$t_{(47)} = 1.74$, $p = 0.09$]. Further, non-parametric test for sex revealed a significant group effect [Kruskal-Wallis: $\chi^2 = 7.04$, df = 2, $p = 0.03$], with more females than males in APOE-ε3-ε3 carriers relative to APOE-ε3-ε2 carriers [Mann-Whitney U: $Z = 2.45$, $p = 0.01$]. There were no differences in the ratio of males and females in APOE-ε3-ε4 carriers relative to APOE-ε3-ε3 carriers [Mann-Whitney U: $Z = 1.63$, $p = 0.10$] or APOE-ε3-ε2 carriers [Mann-Whitney U: $Z = -1.39$, $p = 0.16$]. The study was approved by the ethics committee of the Medical Faculty of the University of Bonn.

METHOD DETAILS

Spatial mnemonic discrimination task

Participants were presented with stimuli of everyday objects that were shown at different locations around a fixation crosshair at the center of the screen (Figure 1A). Stimuli consisted of 160 everyday objects. For each stimulus, participants had to judge whether it was (1) new, (2) old and in the same location (repeat), or (3) old but in a different location (lure). To ensure that the participants would not be able to guess the location of the second presentation of the stimulus, the lure stimulus was randomly rotated with regard to the position of the first presentation of the stimulus around the fixation crosshair at the middle of the screen by either ± 22.5° (lure1), ± 45° (lure2), ± 77.5° (lure3) or ± 90° (lure4). Of the 160 stimuli, 120 were presented twice (40 in the same location for the repeat condition, and 20 * 4 = 80 different locations for the lure conditions) and 40 were presented only once (foils). The stimuli were presented using Presentation software (https://www.neurobs.com/) and back-projected onto an LCD display (OptoStim Medical Research GmbH, Cologne, Germany) that was visible to the participant through a mirror mounted on the MR head coil.

In a rapid event-related design, each stimulus was presented for 2 s, and the mean stimulus onset asynchrony was 5.2 ± 1.8 s (mean ± SD). The mean inter-trial interval between repeated presentations of the same stimulus was 52.5 ± 2.4 s (mean ± SD). Participants completed 2 runs of the fMRI experiment (~13 minutes per run), with a short break between the runs.

MRI data acquisition

A Siemens 7T MAGNETOM research MRI scanner (Siemens Medical Systems, Erlangen, Germany) with a 32-channel head receive coil (single-channel transmit) was used to acquire the MRI data. Before the fMRI session, a whole head T1 MPRAGE volume (TR/TE/TI = 2500/2.91/1200 ms, voxel size = 0.8 * 0.8 * 0.8 mm^3, TA = 4:34 min:s), and 3 fast high-resolution T2-weighted volumes with a reduced field-of-view (55 slices orthogonal to the hippocampus main axis, TR/TE = 8020/76 ms, voxel size = 0.4 * 0.4 * 1.0 mm^3) were acquired at different reference amplitudes (200V, 240V and 280V; TA = 2:58 min:s each) to homogenize the image contrast-to-noise ratio across the field-of-view and to minimize motion artifacts. The 3 T2-weighted images were subsequently coregistered and combined using square root of sum of squares of the 3 images. Each run of the fMRI experiment contained 380 echo planar imaging (EPI) volumes (28 slices in an odd-even interleaved fashion with slice alignment parallel to the hippocampus long axis, TR/TE = 2000/22 ms, voxel size = 0.8 * 0.8 * 0.8 mm^3, parallel imaging acceleration = 4, echo spacing = 1.1 ms (0.275 ms effective echo spacing), partial Fourier = 5/8). The functional volumes were corrected for geometrical distortions using the point spread function mapping method [94] with reduced field-of-view (factor 4) rescan reference acquisition [95]. Total scanning time was 1 hour for each participant.

QUANTIFICATION AND STATISTICAL ANALYSIS

Hippocampal subfields segmentation

Hippocampal subfields were automatically segmented based on both T1 and T2-weighted images using the "Automated Segmentation of Hippocampal Subfields" (ASHS) procedure [48] with an atlas template created by Berron et al. [50] (Figure 2). All resulting images were subsequently checked manually, and edited according to the heuristic rules that created the atlas template [50]. The final images of left and right hippocampal subfields were then co-registered to the mean functional image to create functional regions-of-interest (ROI) mask images for further analyses.

Behavioral analyses

As described above, our experiment contains four types of stimuli: (1) stimuli that were only shown once (foil stimuli), (2) first presentation of subsequently repeated stimuli (new stimuli), (3) old stimuli in the same location (repeat stimuli), and (4) old stimuli in a different location (lure stimuli). Participants' responses were classified into (1) "new," (2) "repeat" (old and in the same location), (3) "lure" (old but in a different location) and (4) no response.

For every participant, the mean proportion of responses (across trials) was calculated in terms of a factorial design with 4 stimulus types by 4 responses (Figure 1B). We did not find any significant APOE genotype group differences for the individual lure conditions (see also Table S2).

fMRI data preprocessing and analyses

FMRI data preprocessing and statistical modeling was performed using SPM12 version 7219 (https://www.fil.ion.ucl.ac.uk/spm/). After removing the first 5 volumes in each run, fMRI data were realigned to the first volume, and smoothed using a 2 mm full-width half-maximum (FWHM) Gaussian kernel. All statistical analyses were performed in the participant's native space. For each participant's 1st level analysis, trials were post hoc sorted according to a factorial design with 4 stimulus type by 4 responses. However, given that there were very little or no trials in some cases, trials from those conditions were collapsed into a single regressor (Figure 1B). In total, the main regressors for the 1st level analysis were: (i) correct foils – foil stimuli with a "new" response, (ii) correct first – new stimuli with a "new" response, (iii) correct repeats – repeat stimuli with a "repeat" response, (iv) repeats "lure" – repeat stimuli with a "lure" response, (v) correct lures – lure stimuli with a "lure" response, (vi) lures "repeat" – lure stimuli with a "repeat" response, (vii) incorrect first presentation – new or foil stimuli with a "repeat," "lure" or no response, and (viii) incorrect second presentation – repeat / lure stimuli with a "new" or no response.

The time-series of data from each voxel were high-pass filtered at 1/128 Hz. Each regressor was entered into the design matrix after convolving each event-related unit impulse (indexing stimulus onsets and stimulus duration of 2 s) with a canonical hemodynamic response function and its first temporal derivative. Six realignment parameters and two session-specific parameters were included as nuisance covariates. The design matrix for each participant was estimated according to the general linear model. For every participant, contrasts for each condition listed above and those reflecting novelty (i.e., correct first > correct repeats), pattern separation (i.e., correct lures > lures "repeat") and relational memory (i.e., correct repeats > repeats "lure") were created and mean (across voxels) parameter estimates for novelty, pattern separation and relational memory effects were extracted for 4 regions of interests (ROIs) bilaterally: Cornu Ammonis 1 (CA1), Cornu Ammonis 3 (CA3), dentate gyrus (DG), and entorhinal cortex (EC). Given that we did not have *a priori* hypotheses regarding hemispheric laterality, we averaged the parameter estimates for each ROI across the 2 hemispheres. To investigate the effects of APOE genotype on either novelty, pattern separation or relational memory effects, repeated-measures of ANCOVAs on the extracted parameter estimates for either novelty (i.e., correct first > correct repeats), pattern separation (i.e., correct lures > lures "repeat") or relational memory (i.e., correct repeats > repeats "lure") effects were performed using "group" (3 levels: APOE-ε3-ε3 versus APOE-ε3-ε4 versus APOE-ε3-ε2) as a between-subjects factor, "ROI" (4 levels: CA1 versus CA3 versus DG versus EC) as a within-subjects factor while controlling for the covariates of "age" and "sex" to account for possible age-related and sex-related effects. The statistical analyses were performed using IBM SPSS Statistics version 22.0 (UNICOM, California, USA). Results were reported using Greenhouse-Geisser correction for inhomeogeneities of covariance.

In a complementary analysis, we modeled the different lure conditions separately. We first created a new general linear model (GLM) with 14 conditions (correct foils, correct first, correct repeats, repeats "lures," correct lure1, lure1 "repeat," correct lure2, lure2 "repeat," correct lure3, lure3 "repeat," correct lure4, lure4 "repeat," incorrect first presentation, and incorrect second presentation). We then extracted the mean parameter estimates (across voxels) related to pattern separation effects for each lure condition in each ROI. For statistical comparison, we computed an ANCOVA with "group" (APOE-ε3-ε3 versus APOE-ε3-ε4 versus APOE-ε3-ε2) as between-subject factor and "lure type" (lure1 versus lure2 versus lure3 versus lure4) and "ROI" (EC versus CA1 versus DG versus CA3) as within-subject factors while controlling for the covariates of "age" and "sex." The statistical analyses were performed using IBM SPSS Statistics version 22.0 (UNICOM, California, USA). Results were reported using Greenhouse-Geisser correction for inhomeogeneities of covariance.

Functional connectivity analyses

To further investigate the role of hippocampal subfields in spatial mnemonic discrimination, we used beta series correlation analyses [56] to calculate how pattern separation affects functional connectivity among EC and hippocampal subfields. In general, functional connectivity in different task conditions can be calculated and compared by fisher-z-transformed correlations of trial-by-trial beta series variability in different conditions. A recent study has demonstrated the similarity between beta series correlation analyses and psychophysiological interaction analyses [96].

For every participant, we first obtained each trial's parameter estimate for each ROI (EC, CA1, DG and CA3) through a GLM including one regressor for that trial and another regressor for all other trials. The temporal derivative of the hemodynamic response function (HRF) was included in the model to account for individual onset variations of the HRF. This process was repeated for every trial and resulted in 280 separate GLMs. For our main analysis, we focused on the functional connectivity effects of pattern separation for correct lures and lures "repeat." Correlations were performed using the parameter estimates of the trials in each condition for each ROI (EC, CA1, DG and CA3) and fisher-z-transformed, thus yielding a 4-by-4 correlation matrix. Given that no directionality (i.e., causation) can be inferred in functional connectivity analyses, only the upper triangle of the correlation matrix was considered. This resulted in 6 unique functional connectivities: (1) EC and DG (EC – DG), (2) DG and CA3 (DG – CA3), (3) CA3 and CA1 (CA3 – CA1), (4) EC and CA1 (EC – CA1), (5) EC and CA3 (EC – CA3), and (6) DG and CA1 (DG – CA1). Finally, effects on pattern separation for each functional connectivity were computed as the difference of the fisher-z-transformed correlations between correct lures and lures "repeat."

To investigate the effects of APOE genotype, repeated-measures ANCOVAs on the effects of APOE genotype on functional connectivity were performed using "group" (3 levels: APOE-ε3-ε3 versus APOE-ε3-ε4 versus APOE-ε3-ε2) as a between-subjects factor and "connectivity" (6 levels: EC – DG versus DG – CA3 versus CA3 – CA1 versus EC – CA1 versus EC – CA3 versus DG – CA1) as a within-subjects factor while controlling for the covariates of age and sex. The statistical analyses were performed using IBM SPSS Statistics version 22.0 (UNICOM, California, USA). Results were reported using Greenhouse-Geisser correction for inhomeogeneities of covariance.